SAND2007-0633J

Defect Structures Produced by Low Temperature Annealing of Pulsed-Laser Deposited Nickel

K. Hattar[1], D. M. Follstaedt[2], J. A. Knapp[2], I. M. Robertson[1]

[1] Materials Science and Engineering, University of Illinois

[2] Sandia National Laboratories

ABSTRACT

The thermal stability of nanograined pulsed-laser deposited nickel was studied by *in-situ* annealing of free-standing films in a transmission electron microscope. The observed grain growth was sporadic and catastrophic as expected for abnormal grain growth. The large grains contained a variety of defects that includes twins, dislocation lines, small dislocation loops, and stacking-fault tetrahedra. This microstructure was developed at annealing temperatures as low as 498 K, and was stable at temperatures as high as 673 K for 20 minutes and subsequently at room temperature for at least 22 months. Possible mechanisms for the formation of these defects during abnormal grain growth are proposed.

INTRODUCTION

Microstructural development of materials via grain growth is generally classified as either normal or abnormal. Normal grain growth is a uniform process in which all grains grow or diminish at a constant rate in an effort to reach an equilibrium size and shape. In contrast, abnormal grain growth is fast and catastrophic, occurring inhomogeneously throughout the material.[1, 2] The driving force for this grain growth is a lowering of the system energy through the decrease in the number of grain boundaries, removal of defects and release of strain energy. Abnormal grain growth, as opposed to normal grain growth, is not fully understood although it appears related to the crystallographic orientation of grains in conjunction with the anisotropy in the surface and grain boundary energies, the grain boundary structure (faceted and non-faceted), strain energy and contamination.[3-6]

Previous studies of grain growth in nanograined thin metallic films have shown that the primary defect formed in association with abnormal grain growth is twins.[7-9] The formation of twins has important consequences for continued grain growth as twin boundaries have low mobility and can decrease the growth rate.[10] Gregg et al.[11] observed during dynamic *in-situ* TEM annealing studies that in some cases the twins must be annihilated before grain growth can occur and in other cases they lengthen with the expanding grain. New twin formation was observed to accompany a burst in grain growth when the growth direction was parallel to the twin boundary normal, but the source of the twinning dislocations in the grain boundary was not determined.

Abnormal grain growth and the formation of annealing twins is not restricted to nanograined metals. In pure metals and alloys with a large grain size (< 100 µm), anomalous grain growth occurs on annealing at temperatures $\geq 0.68T_m$, where T_m is the melting temperature of the material.[12] Booth *et al.*[12] studied grain growth in commercially pure nickel and observed abnormal grain growth. Within these grains were annealing twins, the density of which increased with grain size. This observation suggests that the generation of annealing twins is not governed strongly by the stacking-fault energy as Ni has a high stacking-fault energy for a face-centered cubic material, 125 mJ m^{-2}.[13] It has been suggested that abnormal grain growth occurs when the boundaries are faceted through the movement of steps and this distinguishes the two growth modes.[14] Mahajan *et al*.[15] proposed that the annealing twins were created by the emission of the required Shockley partial dislocations from growth accidents on the migrating grain boundary. As the number of growth accidents likely would increase with the velocity of the migrating grain boundary, more annealing twins would be expected for higher velocities.[15]

In this manuscript, the emphasis is on the formation of defects in large grains developed in pulsed-laser deposited nickel during abnormal grain growth and the stability of these defects over time and temperature. Details of the dependence of the abnormal grain growth on annealing temperature, annealing time, film thickness, surface roughness, and electron beam will be presented elsewhere.[16]

EXPERIMENTAL PROCEDURE

Nanograined nickel thin films were grown on <100> rock salt substrates to thicknesses of 50, 80, and 150 nm by using the pulsed-laser deposition technique. The growth chamber achieved a base pressure of $2x10^{-7}$ Torr, with the pressure rising to about five times higher during the laser pulses. The KrF laser pulse operated at a wavelength of 248 nm with a pulse width of 34 ns full-width half-maximum, a pulse rate of 35 Hz, and a power density of 1-2 J cm^{-2}. Plasmas released from the target and deposited at the sample surface typically have energies in the 1-5 eV/atom range. These conditions resulted in a film growth rate of about 0.25 nm s^{-1}. As discussed in detail in Ref.[17], a particle filter was used to minimize the number of molten droplets that were deposited onto the specimen, which form "splats" of larger-grained material in the nanocrystalline matrix.

To produce free-standing samples for the *in situ* transmission electron microscopy (TEM) annealing investigation, a copper grid was adhered to the deposited film and the rock salt support was dissolved in water. The free-standing nanograined PLD nickel thin film was annealed *in situ* in a Philips CM20T TEM operating at 200 kV. Notably, the accelerating voltage is below that needed to create Frenkel pairs in Ni.[18] The temperature of the Gatan single-tilt heating stage (Model 628-Ta) used in these experiments was determined to be accurate to within a few degrees. However there is greater uncertainty about the actual temperature of the area being examined as it is not in intimate contact with the heating element. The temperature quoted is the heater temperature and should be taken as a maximum as there was no method for independently determining the actual specimen temperature. Specimens were annealed until significant grain growth was observed at nominal temperatures ranging from 498 K to 673 K and times ranging from 10 min. to 840 min. The stated temperature is probably more accurate for longer anneal times as the temperature across the specimen will equilibrate. The resulting microstructures were then characterized using conventional diffraction contrast imaging techniques.

EXPERIMENTAL RESULTS

The as-deposited microstructure of the films had an average grain size of 6 nm with a limited grain size distribution, 2 nm to 16 nm, as can be seen in the bright-field micrograph of an 80 nm thick film presented in Figure 1. The grains are randomly oriented with a few samples showing limited <100> preferred texture due to the rock salt substrate. Widely-spaced large nickel "splats" (deposited molten droplets), like that indicated in Figure 1, provide fiducial marks to enable the same region to be identified repeatedly during the course of the experiments. Preliminary high-resolution studies of the as-deposited grains suggest that the boundaries between the nanograins are high-angle with no evidence for porosity; this finding is consistent with previous observations of this material. No defects were observed in the as-deposited nanograined structure although dislocations have been reported in strained nanograined pulsed-laser deposited nickel.[19].

On heating, the microstructure developed in an erratic and catastrophic manner that is typical of abnormal grain growth. Irrespective of film thickness, all films exhibited abnormal grain growth at temperatures as low as 548 K, with the faster reacting 150 nm-thick film showing abnormal growth down to 498K. This resulted in the formation of large grains up to a micrometer in size distributed randomly throughout the film. These grains were enclosed in a matrix of nanograins that had experienced little or no growth. Representative examples of abnormally large grains are presented in Figures 2 and 3.

The microstructure depicted in Figure 2 shows the results of annealing a 150 nm-thick film at a temperature of 498 K for 840 min. The anneal produced a large grain that appears to be approximately elliptical with the major and minor axes being 450 and 350 nm, respectively. A complex defect structure is evident in the grain. The magnified image of the boxed area, seen in Figure 2B, shows dislocations and stacking-fault tetrahedra, which appear as triangular defects, coexisting in the grain. The presence of dislocation half-loops emerging from the grain boundary indicates that the boundary is the origin of the dislocations.

The micrographs presented in Figure 3 show a 700 nm-sized grain existing in a 150 nm-thick film following an anneal at 548 K for 20 minutes. The grain is twinned, as seen by the contrast change between the two halves in Figure 3A. The twinned orientation is confirmed with the electron diffraction pattern shown in the inset. The microstructure within both regions includes dislocations (arrowed defects), stacking-fault tetrahedra (circled defects), and a planar defect (enclosed in an ellipse) in Figure 3B. The nature of the planar defect was not determined and could be a twin that has propagated only part way through the grain. In this region more than one grain has grown; the upper grain impinging on the twinned grain has also grown but to a lesser extent. As in the other examples, this grain was also populated by defects.

The size of each tetrahedron was estimated from measurement of the length of the triangle obtained in kinematical imaging conditions. Although a one-to-one correspondence between the image and the defect size has not been established,[20] assessing the size distribution provides insight to the number of vacancies that are needed to create the defects. The size distribution of the tetrahedra in the 150 nm-thick film created by the annealing conditions of 498K for 840 min, obtained from the microstructure of the grain shown in Figure 2, is presented in Figure 4. The line length of the tetrahedra varies from 1.5 nm to as large as 11.9 nm, with the average size being 5.6 nm. For this grain, the total volume of the stacking-fault tetrahedra is 1,400 nm^3, which is 0.002% of the total grain volume of 0.07 μm^3. The number of vacancies, N, that would be needed to occupy a tetrahedron of edge length L can be calculated from the expression $N = \frac{2L^2}{\sqrt{3}\, a_o^2}$, where a_o is the lattice parameter, which is 0.354 nm for Ni. The average number of vacancies per stacking-fault tetrahedra is 289 and ranges from 20 vacancies for a tetrahedron of length L = 1.5 nm to 1305 nm for one with a length of 11.9 nm.

Similar defect microstructures were produced by annealing at 673 K, and these defects were stable at this temperature for at least 20 min. The defects were also stable against room temperature aging for at least 22 months. This room temperature stability is evident from comparison of the bright-field images presented in Figure 5, which show the same area presented in Figure 3 but after six months and 15 months aging at room temperature. Although the same area of the film was located in these extended aging studies, it is not possible to obtain the exact same diffraction conditions, which affects the appearance of the defect structures. However, by comparing the images it is obvious there has been no major change in the grain morphology and the same defects still exist. The planar defects, stacking-fault tetrahedra, and small dislocation loops remaining after 15 months can be seen in Figure 5C. Recent imaging shows that the twins, dislocations and stacking-fault tetrahedra are still present after 22 months.

DISCUSSION

Uniformly thick nanograined Ni films produced by pulsed-laser deposition that were annealed in the transmission electron microscope exhibited abnormal grain growth. The resulting large grains contained a population of twins, dislocations, small dislocation loops and stacking-fault tetrahedra at the annealing temperature. This result is in contrast to findings in nanograined Ni produced by electrodeposition in which abnormal grain growth occurred in the temperature range from 349 to 562K, but no defect structure was reported in the abnormally large grains, although twins can be seen in the published images.[3, 4] It is also at variance with the microstructure of other annealed nanograined FCC thin films, which is generally dominated by twins.[7-9, 11] These findings suggest the formation of this defect population was not determined by the metal itself but was likely a consequence of the deposition process and initial nanostructure.

A key question to be addressed is the origin of the defects. The presence of dislocation half-loops emerging from grain boundaries indicates that the line dislocations are likely generated from the grain boundaries; see Figures 2B. The dislocation source was not identified but the emission may be a consequence of the atomic rearrangements occurring in the migrating grain boundary, which may have been assisted by local strain incompatibilities between the growing grain and the surrounding nanograined structure.

Annealing twins were produced in some of the large grains, as in Figure 3, and although they generally extended across the grain there were some exceptions where twins ended in the grain. The appearance of twins in Ni is not restricted to electron transparent pulsed-laser deposited material as annealing twins have been observed in large grains produced by abnormal grain growth in commercially pure Ni with a starting grain size less than 10^{-4} m.[12] Thus, starting with nanograins is not a necessary condition for the formation of annealing twins although it may influence the twin density. Twin generation is not related only to growth defects as deformation twins have been reported in coarse-grained Ni during deformation *in-situ* in the transmission electron microscope[21] and in post-deformation TEM examination of nano-grained Ni.[22]

The nature of the stacking-fault tetrahedra is assumed to be vacancy,[23] which raises the issue about the origin of the vacancies needed to create the observed density of tetrahedra. High concentrations of vacancies can be obtained by rapid quenching from temperatures near T_m,[24, 25] by irradiation with energetic particles,[20, 26] and possibly by high strain-rate (10^8 s^{-1}) deformation.[27, 28] The maximum annealing temperature in this study was 673K (=0.39T_m) which would generate only 0.1 ppm thermal vacancies,[29] much less than the vacancy content determined above. This low concentration of thermal vacancies and the fact that the tetrahedra were observed while at the annealing temperature eliminates this mechanism. Stacking-fault tetrahedra have been reported to form in Ni following 840 keV Ni ion irradiation at room temperature[26] whereas vacancy loops are produced on irradiation with lower energy ions.[20] Molecular dynamics computer simulations suggest that tetrahedra are formed near grain boundaries in nanograined nickel for implantations with 10 keV ions,[30] but this has not been verified experimentally. As the Ni plasma impacting the growing film has an energy in the range of 1-5 eV per atom, which can cause surface effects only, an irradiation mechanism can be eliminated. The strain-based mechanism can be eliminated readily as the sample did not experience any high strain-rate deformation. Therefore, it can be concluded that none of these mechanisms is appropriate to produce vacancies in the current investigations.

The stacking-fault tetrahedra are observed only in abnormally grown grains, suggesting that either the faults themselves or the vacancies that form them are generated and released from the migrating grain boundary. The former is unlikely as the complete three-dimensional defect would have to form in the grain boundary and be left behind as it moves, although such a mechanism has been reported previously to account for the generation of large defects in a Cu-Si alloy.[31] Such a mechanism would imply that a correlation between the spatial distribution of the tetrahedra and the grain boundary migration rate should exist, but no obvious correlation was found in the present experiments. Vacancies and even vacancy clusters could be created as debris by the advancing grain boundary much in the same way they are created during dislocation motion. This mechanism for generating vacancies is similar to that proposed by Jahn and King [32] to account for the observation of stacking-fault tetrahedra in the wake of a migrating grain boundary in a copper-zinc alloy in the limited regime of temperature between 0.3T_m and 0.5T_m, and grain boundary migration rates between $3\text{x } 10^6 \text{ nm s}^{-1} \leq V \leq 1\text{x } 10^{-1} \text{ nm s}^{-1}$.

The temperature range for the current experiments was $0.29T_m$ to $0.39\ T_m$ and the boundary migration rate is between 6 nm s^{-2} and 5.5×10^{-3} nm s^{-1}, putting the current observations at the lower limits reported by Jahn and King [32]. However, in our case it is postulated that the vacancies are generated directly from the imperfect nature of the grain boundaries produced by pulsed-laser deposition. The high-angle grain boundaries have a lower atomic density than the fcc Ni lattice and are thus a potential source of vacancies when they are incorporated into the growing grains. The fact that this defect structure was observed only for pulsed-laser deposited Ni and not for electrodeposited Ni is an indicator that the defects are generated as a consequence of the initial structure produced by the processing.

The mechanism of formation of a tetrahedron from a vacancy population was not observed in this study. It is possible that vacancies first agglomerated into a Frank loop which then dissociated according to the Silcox-Hirsch mechanism[33] to a stacking-fault tetrahedron or that the tetrahedron formed by a clustering mechanism in which a stable nucleus grows to become visible by the accumulation of vacancies.[13, 34] The latter mechanism would be aided by the presence of other defects and the nuclei could be stabilized by oxygen, which is present in the deposited films.[17] The formation of a stacking-fault tetrahedron, according to the energy calculations of Zinkle *et al.*[35] for nickel with a stacking-fault energy of 150 mJ m^{-2}, is favored at small sizes. The calculations predict a stacking-fault tetrahedron would be the stable defect for about 300 vacancies, which corresponds to a line length of 5.7 nm. Between 300 and 1000 vacancies, the energetically favored defect will be a Frank loop with a radius of 2.9 nm to 5.9 nm, respectively. At larger loop sizes, the Frank loop will unfault to a perfect loop. It is therefore not surprising that stacking-fault tetrahedra are produced but the predicted maximum size suggests the larger tetrahedra observed in this study (up to 11.9 nm) may need to be stabilized, perhaps by the oxygen impurities.[17]

The defect structure remains stable on aging at 673K for 20 minutes. Singh *et al.*[28] have compared the annealing behavior of stacking–fault tetrahedra in Au and Cu that were produced by annealing of a quenched structure and by ion implantation, respectively. Annealing of the stacking-fault tetrahedra in gold occurred at temperatures above 758K and in copper at temperatures above 573K. The trend was for smaller tetrahedra to be annihilated first, as evidenced by a shift in the peak of the size distribution to higher sizes with annealing. The maximum size of the stacking-fault tetrahedra appeared to remain fairly constant with annealing, with the maximum size being between 12 and 14 nm, and 6 and 8 nm in gold and copper, respectively. According to the energetics calculations by Zinkle *et al.*[35] the transition between a stacking-fault tetrahedron and a Frank loop should occur for approximately 700 and 1000 vacancies in Au and Cu, respectively, which corresponds to sizes of 10 nm and 10.6 nm. Thus the discrepancy between observed and calculated maximum sizes for tetrahedra in Ni is similar to those found for Au and Cu.

CONCLUSIONS

On annealing pulsed-laser deposited nickel *in situ* in an electron microscope abnormal grain growth was observed. These abnormally large grains contained a significant density of defects, twins, line dislocations, and stacking-fault tetrahedra. The origin of the dislocations is from grain boundary sources as evidenced by the emerging half-loops. It is also proposed that the vacancies for the tetrahedra are generated from the excess free volume in the grain boundaries of the deposited material. The defect structure was stable against annealing at temperatures up to 673 K and persists for at least 22 months at room temperature, which are consistent with observations of the thermal stability of defects in other systems.

ACKNOWLEDGMENTS

This research was partially supported by a grant from National Science Foundation Division of Materials Research, Award No. 02037400 (IMR and KH). The work at Sandia was supported by the Division of Materials Sciences and Engineering, Office of Basic Energy Sciences, of the U.S. Department of Energy. Sandia is a multi-program laboratory operated by Sandia Corporation, a Lockheed Martin Company, for the United States Department of Energy's National Nuclear Security Administration under contract DE-AC04-94AL85000. A portion of this research was carried out in the Center for Microanalysis of Materials, University of Illinois, which is partially supported by the U.S. Department of Energy under grant DEFG02-91-ER45439. The authors would like to thank Prof. A. H. King and Dr. R. G. Hoagland for their insightful discussion.

REFERENCES

[1] Rios PR. Materials Science Forum 1996; 204-206: 247.
[2] Yamazaki Y and Watanabe T. Materials Science Forum 2nd International Conference on Grain Growth in Polycrystalline Materials, 17-20 May 1995 1996; 204-206: 257.
[3] Klement U, Erb U and Aust KT. Second International Conference on Nanostructured Materials, 3-7 Oct. 1994
Nanostructured Materials. 6, 1995 pp. 581.
[4] Klement U, Erb U, El-Sherik AM and Aust KT. Materials Science & Engineering A 1995; A203: 177.
[5] Nabarro FRN. Scripta Materialia 1998; 39: p 1681.
[6] Thompson CV and Carel R. Materials Science Forum 1996; 204-206: 83.
[7] Greiser J, Mullner P and Arzt E. Acta Materialia 2001; 49: 1041.
[8] Paik J-M, Park Y-J, Yoon M-S, Lee J-H and Joo Y-C. Scripta Materialia 2003; 48: 683.
[9] Weihnacht V and Bruckner W. Thin Solid Films 2002; 418: 136.
[10] Masteller MS and Bauer CL. Acta Metallurgica 1979; 27: 483.
[11] Gregg JA, Hattar K, Lei C-H and Robertson IM. Mater. Res. Soc. Symp. Proc. 907E, 2005 pp. 0907-MM06-03.
[12] Booth M, Randle V and Owen G. Journal of Microscopy 2005; 217: 162.
[13] Hirth JP and Lothe J. *Theory of Dislocations*. McGraw-Hill Inc. New Yourk: 1968.
[14] Rath BB, Pande CS and Imam MA. Proceedings of Advances in Twinning. 1999 TMS Annual Meeting, 28 Feb.-4 March 1999. TMS - Miner. Metals & Mater. Soc, 1999 p. 3-12 BN - 0 87339 430 5.
[15] Mahajan S, Pande CS, Imam MA and Rath BB. Acta Materialia 1997; 45: 2633.
[16] Hattar K, Follstaedt DM, Knapp JA and Robertson IM. unpublished
[17] Knapp JA and Follstaedt DM. Journal of Materials Research 2004; 19: 218.
[18] Williams DB and Carter CB. *Transmission electron microscopy*. Plenum Press. New Yourk: 1996.
[19] Shan Z, Stach EA, Wiezorek JMK, Knapp JA, Follstaedt DM and Mao SX. Science 2004; 305: 654.
[20] Robertson IM, Vetrano JS, Kirk MA and Jenkins ML. Philosophical Magazine A: 1991; 63: 299.
[21] Robertson IM. Philosophical Magazine A 1986; 54: 821.
[22] Wu X, Zhu YT, Chen MW and Ma E. Scripta Materialia 2006; 54: 1685-1690.
[23] Kojima S, Satoh Y, Taoka H, Ishida I, Yoshiie T and Kiritani M. Philosophical Magazine A 1989; 59: 519.
[24] Moya G. Acta Metallurgica 1975; 23: 289.
[25] de Jong M and Koehler JS. Physical Review 1963; 129: 49.
[26] Nita N, Schaeublin R, Victoria M and Valiev RZ. Philosophical Magazine 2005; 85: 723.
[27] Kiritani M, Yasunaga K, Matsukawa Y and Komatsu M. Electron Microscopy: Its Role in Materials Science, Mar 2-6 2003. Minerals, Metals and Materials Society, Warrendale, PA 15086, United States, 2003 p. 71.
[28] Singh BN, Golubov SI, Trinkaus H, Edwards DJ and Eldrup M. Journal of Nuclear Materials 2004; 328: 77.

[29] Smedskjaer LC, Fluss MJ, Legnini DG, Chason MK and Siegel RW. Journal of Physics F (Metal Physics) 1981; 11: 2221.
[30] Samaras M, Derlet PM, Van Swygenhoven H and Victoria M. Philosophical Magazine 2003; 83: 3599.
[31] Clarebrough LM and Forwood CT. Physica Status Solidi A 1987; 104: 51.
[32] Jahn RJ and King AH. Philosophical Magazine A 1986; 54: 3.
[33] Silcox J and Hirsch PB. Philosophical Magazine 1959; 4: 72.
[34] Kuhlmann-Wilsdorf D. Acta Metallurgica 1965; 13: 257.
[35] Zinkle SJ, Seitzman LE and Wolfer WG. Philosophical Magazine A 1987; 55: 111.

Figure captions

Figure 1 Initial nanostructure of fcc grains in an 80 nm-thick PLD Ni film, with inserted selected area diffraction pattern.

Figure 2 A) A large abnormal grain in a matrix of nanograins in 150 nm-thick PLD Ni film resulting from annealing at 498 K for 14 hrs. B) A variety of defects in the enlarged region of the image. Examples of stacking-fault tetrahedra are circled and dislocations are arrowed.

Figure 3 A) A large twinned grain in a 150 nm-thick film after annealing at 548 K for 20 min. Inset: Electron diffraction pattern demonstrating the twinned orientation of the two halves of the grain. B) Defect structure: stacking-fault tetrahedra are circled, an ellipse is drawn around a planar defect, and dislocations are arrowed.

Figure 4 Stacking-fault tetrahedra size distribution.

Figure 5 A) Defects located in the same grain after 6 months, B) Defects in the same grain 15 months after aging at room temperature. C) High magnification micrograph of the same grain after 15 months.

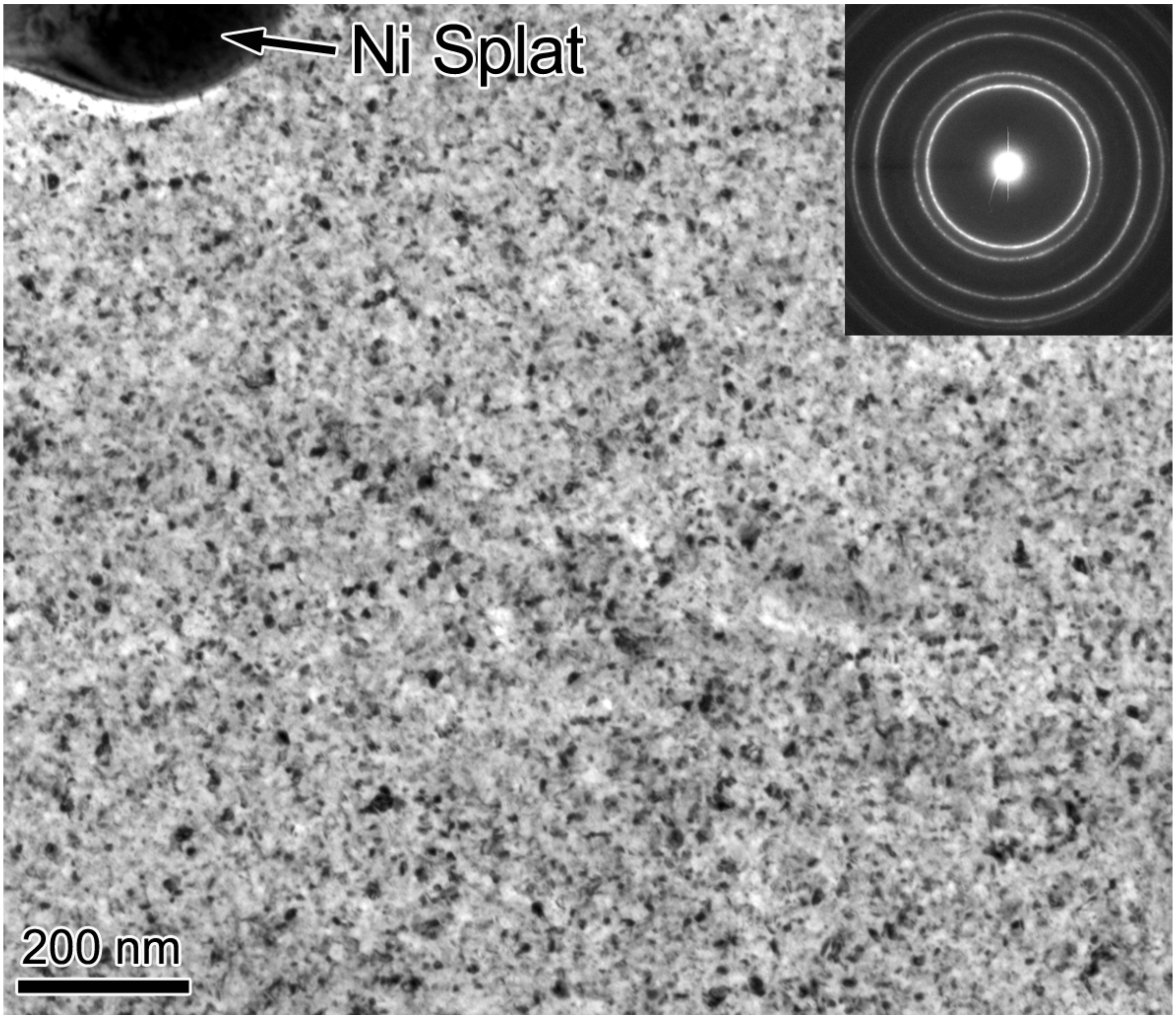

Figure 2 Initial nanostructure of fcc grains in an 80 nm-thick PLD Ni film, with inserted selected area diffraction pattern.

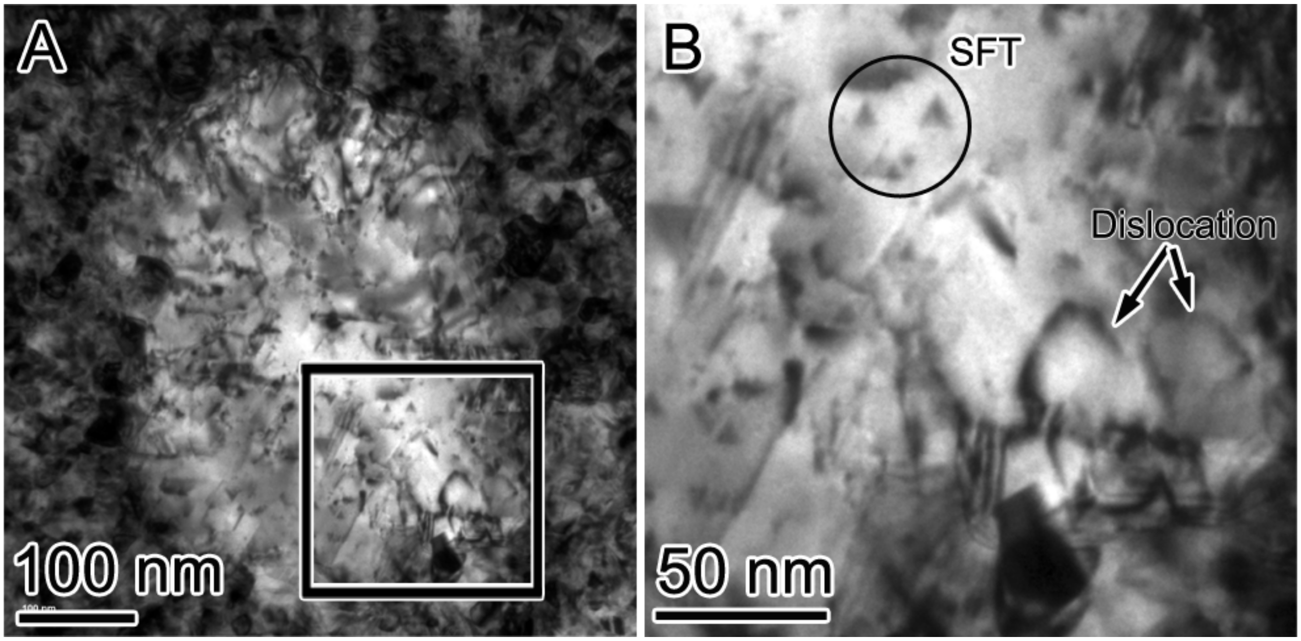

Figure 2 A) A large abnormal grain in a matrix of nanograins in 150 nm-thick PLD Ni film resulting from annealing at 498 K for 14 hrs. B) A variety of defects in the enlarged region of the image. Examples of stacking-fault tetrahedra are circled and dislocations are arrowed.

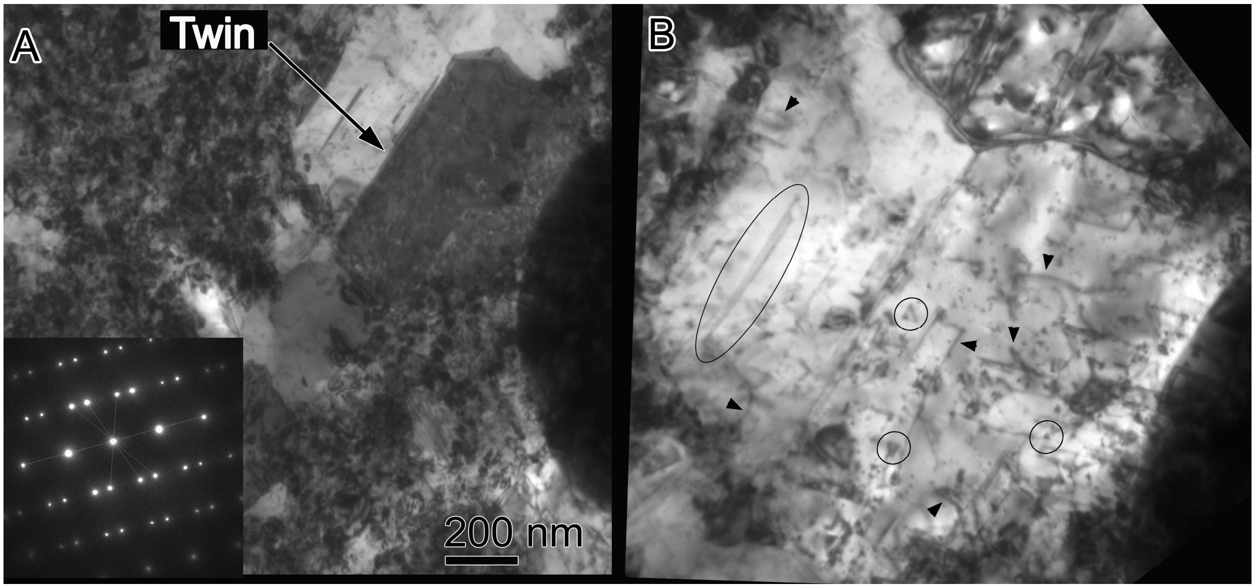

Figure 3 A) A large twinned grain in a 150 nm-thick film after annealing at 548 K for 20 min. Inset: Electron diffraction pattern demonstrating the twinned orientation of the two halves of the grain. B) Defect structure: stacking-fault tetrahedra are circled, an ellipse is drawn around a planar defect, and dislocations are arrowed.

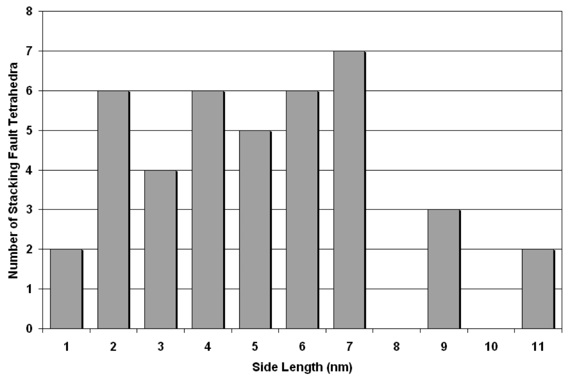

Figure 4 Stacking-fault tetrahedra size distribution.

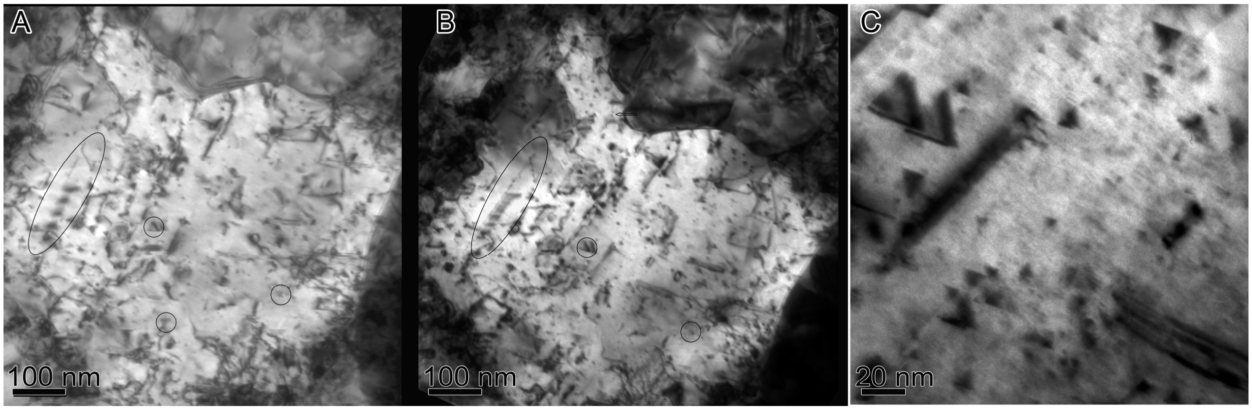

Figure 5 A) Defects located in the same grain after 6 months, B) Defects in the same grain 15 months after aging at room temperature. C) High magnification micrograph of the same grain after 15 months.